Magazine of Civil Engineering

ISSN 2712-8172

journal homepage: http://engstroy.spbstu.ru/

DOI: 10.34910/MCE.107.6

Algorithm of correcting bimoments in calculations of thin-walled bar systems

I.N. Serpik*, R.O. Shkolyarenko
Bryansk State University of Engineering and Technology, Bryansk, Russia
**E-mail: inserpik@gmail.com*

Keywords: frames, thin-walled bars, restrained torsion, bimoments, bar connection nodes, finite element method, iterative process

Abstract. An algorithm developed for enhancing the accuracy of the calculation of frames formed by thin-walled open-section bars is presented. The existing bar models for analysis of frame systems consisting of open-section bars subjected to restrained torsion require improvement. Some authors have shown that the traditional premise of a balance of bimoments at the junction of such bars may be violated in many cases. The methodology described in this article is formulated on the condition that the disbalance on bimoments in connecting nodes of rods reinforced with transversal ribs can be taken into account on the basis of the eccentric moments transfer on the bar junctions. An approach based on the Lagrange variational principle to the construction of equations of finite element analysis while taking into account such disbalances is proposed. Herewith, some additional nodal bimoments are introduced. They allow us to correct the solution of the problem and do not affect the global stiffness matrix of the finite element system. A presented rapidly converging iterative process makes it possible to estimate the values of such bimoments. The performance of the suggested methodology has been illustrated via an example of the calculation of frames made of I-beams and U-beams. The comparison of the results of bimoments definition using the developed bar calculation schemes and shell models have shown that the suggested algorithm allows describing the disbalance of bimoments in bar connection nodes to a fairly high degree of precision for practical goals. This result may have significant importance for improving computer modelling of deformations of the thin-walled open-section bar structures.

1. Introduction

Calculations of thin-walled bars and bar systems while taking into account torsion can be performed efficiently using shell models [1–3] or three-dimensional analysis [4]. However, the implementation of such approaches for real constructions, especially for carrying out multivariant calculations is often associated with fairly lengthy computational process working hours. Using bar design models is more promising for engineering practice.

It should be noted that the modern regulatory requirements for steel structures (Russian State Standard SP 16.13330.2017 "Steel Structures. Updated revision of SNiP II-23-81*") stipulates consideration of bimoments when determining normal stresses in bar cross sections. First of all, this factor can be significant for thin-walled open-section bars if there is restrained warping of cross sections during torsion. Theories of calculating thin-walled bars while taking into account restrained torsion within a one-dimensional approach are described in sufficient detail in scientific literature. The best known theory is the shear theory by A.A. Umansky, the shearless theory by V.Z. Vlasov, and the semi-shear theory by V.I. Slivker [5–7]. Much attention was also paid to the development of bar finite elements for thin-walled bars based on models of various types [8–26].

Several approaches to taking into account restrained torsion using the finite-element method based on bar models are presented in [8]. For the shearless theory, a double-node open-section finite element has been considered with approximation of rotation angle using Hermite cubic polynomials. For the semi-shear theory,

Serpik, I.N., Shkolyarenko, R.O. Algorithm of correcting bimoments in calculations of thin-walled bar systems. Magazine of Civil Engineering. 2021. 107(7). Article No. 10706. DOI: 10.34910/MCE.107.6

© Serpik, I.N., Shkolyarenko, R.O., 2021. Published by Peter the Great St. Petersburg Polytechnic University.

This work is licensed under a CC BY-NC 4.0

some stiffness matrices of open- and closed-section thin-walled bar finite elements have been constructed for three models of description of rotation angles and measures of warping of cross sections: linear approximations of rotation angle and measure of warping in a double-node finite element, quadratic approximation of rotation angle and linear approximation of measure of warping in a three-node finite element, quadratic approximations of rotation angle, and measure of warping for a three-node finite element. In [9] precision of finite-element analysis has been studied using the shearless and semi-shear theories for thin-walled open-section bars. A double-node finite element constructed within the shearless theory with cubic approximation of rotation angle and offset of the line along which the approximation of longitudinal displacements was performed is considered during analysis of deformations of plate-and-bar systems in [10]. In [11] an issue of calculation has been elaborated using a finite-element method for thin-walled open-section curved bars.

Different variants of thin-walled open-section finite elements have been constructed using analytical solutions of differential equations [13, 14, 19, 20]. In [21] an approach has been considered for implementation of the shearless theory in finite-element analysis using a double-bar finite element. By introduction of the main and dummy bar, a possibility is ensured to set the seventh degree of freedom in the node, which allows taking into account the restrained torsion within the existing software systems which traditionally use six degrees of freedom in a node.

However, the frame calculation methodology taking into account the strain warping needs to be further developed. The most widely used supposition is that presented in [6], concerning the balance of bimoments and the equality of measures of warping at bar junctions. The analysis on this basis of flat-space frames made of open-section bars [27, 28] was considered. However, [29, 30] note that such conditions are often violated, and bar interaction behavior depends significantly on their connection design. This problem can be fundamentally solved using a combined approach, where bar finite elements are introduced outside the junction node zone, and the junction strains are described using shell finite elements [31]. At the same time, the structural designs are complicated significantly in this case.

In [32–34] the regularity of the transfer of internal force factors in bar connection nodes equipped with transversal ribs has been studied in respect to disbalance of bimoments. It has been noted that such disbalance can be taken into account based on the consideration of eccentric moments transfer in the bar junctions. In [34] a step-by-step scheme for accounting of this phenomenon has been introduced within the finite element method by changing position of auxiliary linking elements between the bars. Fairly high precision of this methodology has been illustrated by an example of calculation of thin-walled structures consisting of two and three channel bars. At the same time, this approach supposes re-forming the matrix of a system of resulting equations during each iterative process step.

The aim of this work is the development of a rapidly converging, iterative scheme for accounting of physical prerequisites of [32–34] by introducing some additional nodal bimoments which do not influence the global stiffness matrix of the finite element method and do not require any changes of positions of auxiliary connection links.

2. Methods

2.1. Definition of the bimoment relationship condition

Let us consider a linearly elastic frame made of thin-walled open-section bars equipped with transversal ribs. We will assume that the frame bar has a longitudinally uniform cross-section and can be generally subjected to tension-compression, cross bending in two principal planes, and restrained torsion. Let us deem Vlasov's restrained torsion theory to be true for bars. We will discretise the object using thin-walled bar finite elements placing nodal points in the bending centers of their extreme cross sections. Herewith, we initially form bar system S, where thin-walled bars T are located between nodes U of the finite-element model, and the external load is reduced to such nodes. In system S bars T can be directly pairwise connected on nodes U or using stiff inserts D (Fig. 1). Let us assume that measures of warping cross sections are transferred through such inserts without any changes. The potential energy for bar T (Fig. 2) can be written as

$$\Pi = \frac{1}{2}\int_0^l \left(N\varepsilon_x + M_x\chi_x + M_y\chi_y + M_\theta\theta + B_\omega \frac{d\theta}{dx} \right) dx - \\ - \sum_{i=1}^{2} \left(R_{xi}u_i + R_{yi}v_i + R_{zi}w_i + m_{xi}\phi_{xi} + m_{yi}\phi_{yi} + m_{zi}\phi_{zi} + B_{\omega i}\theta_i \right), \quad (1)$$

where l is the bar length,

N is a longitudinal force,

$\varepsilon_x = \dfrac{\partial u}{\partial x}$ is the strain per unit of length along axis Ox,

u is the cross section center-of-gravity displacement vector projection on axis Ox,

M_y, M_z are the bending moments in relation to the main central axes Oy, Oz of cross section,

$\chi_y = \dfrac{d^2 w}{dx^2}$, $\chi_z = \dfrac{d^2 v}{dx^2}$ are the bar bending strains in relation to axes Oy and Oz,

w, v are the cross section center of bending displacement vector projections on axes Oz and Oy,

M_θ is a pure torsion moment,

$\theta = d\phi_x / dx$ is a measure of warping,

ϕ_x is the cross section rotation angle relative to axis Ox,

B_ω is a bimoment,

R_{xi} is the force acting on the bar along axis Ox in cross section from node i $(i = 1, 2)$,

u_i, v_i, w_i are the values u, v, w in node i,

R_{yi}, R_{zi} are the forces applied to the bar from node i in the center of bending P_i of cross section H_i,

$m_{xi}, m_{yi}, m_{zi}, B_{\omega i}$ are the axial moments and a bimoment acting on the bar from node i,

$\phi_{xi}, \phi_{yi}, \phi_{zi}$ are the cross section H_i rotation angles relative to axes Ox, Oy, Oz,

θ_i is the measure of warping for node i.

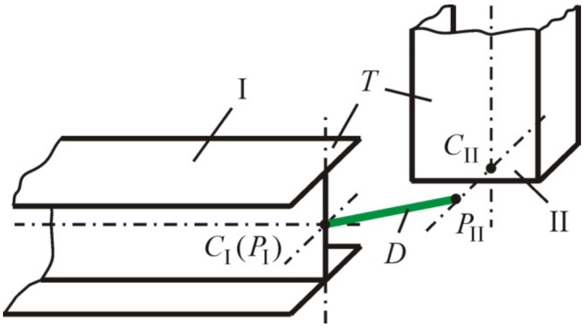

Figure 1. Example of introduction of a stiff insert D between nodes of thin-walled bars I and II: C_I, C_II, P_I, P_II are respectively centers of gravity and centers of bending of cross sections of bars to be joined.

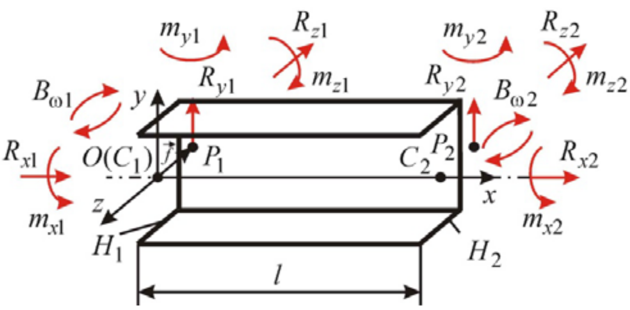

Figure 2. Bar T of system S by the example of a channel section: H_1, H_2 are the nodal cross sections with centers of gravity C_1, C_2 and bending centers P_1, P_2; $\vec{f}$ is a vector connecting the cross section center of gravity and center of bending.

Let us present the bimoment of node i as

$$B_{\omega i} = B_{\omega}\left(m_{yi}\right) + B_{\omega}\left(m_{zi}\right) + \tilde{B}_{\omega i} + B_{R\omega i}\alpha_{Ri}, \quad (2)$$

where $B_{\omega}\left(m_{yi}\right)$, $B_{\omega}\left(m_{zi}\right)$ are bimoments created in such a node by moments m_{yi}, m_{zi} respectively with due allowance for the actual conditions of their application to the bar,

$\tilde{B}_{\omega i}$ is a bimoment which we will treat as one conditioned via transfer of bimoments from neighboring bars,

$B_{R\omega i}$ is an external bimoment applied in cross section H_i,

α_{Ri} is the relative share of the bimoment $B_{R\omega i}$ taken up by the finite element.

For example, as shown by calculations [33], for I-section (Fig. 3a), connected with some bar L through flange Π, moment m_{yi} from such a bar will be actually transferred in the plane spaced from plane $C_i xz$ approximately at distance $d = 0.6h_{\alpha}$, where h_{α} is half the distance between the middle planes of the flanges. Let us introduce a self-balanced system of force couples acting in plane $C_i xz$ with moments m_A, m_B provided $\left|m_A\right| = \left|m_B\right| = \left|m_{yi}\right|$. Herewith, moment m_A bends the bar, and the self-balanced system of moments m_{yi}, m_B will be treated as a bimoment $B_{\omega}\left(m_{yi}\right)$, the modulus of which

$$\left|B_{\omega}\left(m_{yi}\right)\right| = \left|m_{yi}\right| d. \quad (3)$$

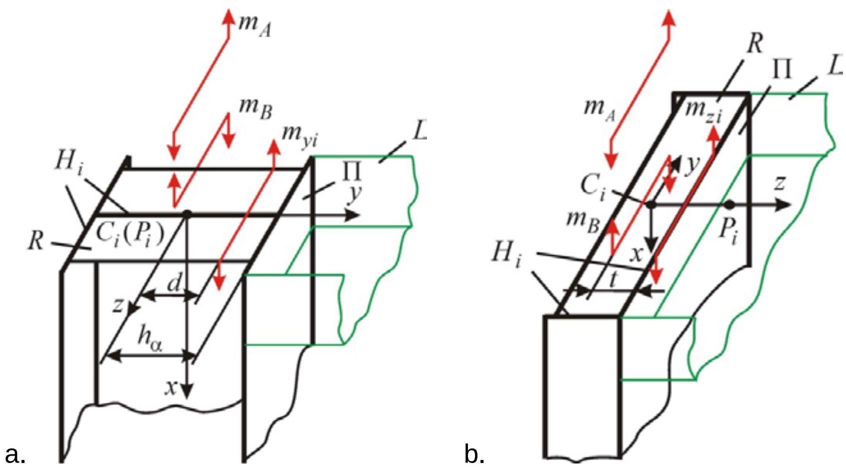

Figure 3. Transfer of a moment to I-section (a) and channel section (b): R are the transversal ribs.

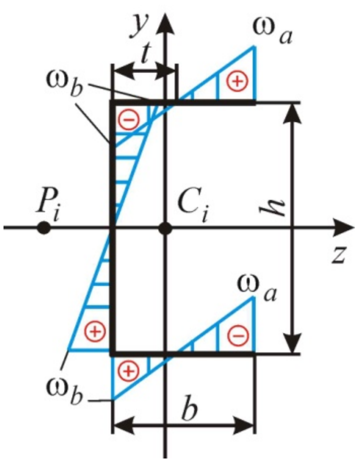

Figure 4. Principal sectorial coordinates for a channel section.

For channel section (Fig. 3b) during transfer of moment m_{zi} through the channel web Π it can be approximately assumed that it acts in the middle plane of this web [34]. Let us consider moments m_A, m_B, which are equal in absolute value to moment $|m_{zi}|$ and which are in the plane parallel to plane $C_i xy$ and spaced from the middle plane of the channel web Π by distance t. This distance corresponds to the position of points with zero values of principal sectorial coordinates [6] shown in Fig. 4, where ω_a, ω_b are coordinates depending on the dimensions of the cross section.

Then we get

$$\left|B_\omega\left(m_{zi}\right)\right| = \left|m_{zi}\right| t. \tag{4}$$

According to the researches of [33, 34], we assume that in system S at the junction of two or more bars T connected directly on nodes U or using inserts D the following relationship on bimoments is fulfilled:

$$\sum_{k=1}^{k_o} \left(\tilde{B}_{\omega i(k)} + B_{R\omega i(k)}\right)^* = 0, \tag{5}$$

where k_o is the number of bars to be connected,

$\tilde{B}_{\omega i(k)}$, $B_{R\omega i(k)}$ are magnitudes $\tilde{B}_{\omega i}$, $B_{R\omega i}$ for bar k in the connecting node,

$(\,)^*$ is a designation indicating that the signs of the bimoments in brackets are adjusted according to Fig. 5.

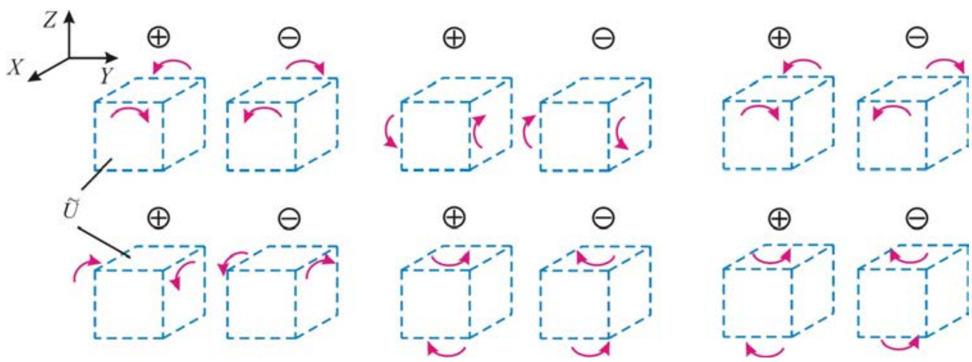

Figure 5. Sign rules for bimoments in terms of their action on connecting nodes $\tilde{U}$ when applied relative to axes *X* и *Y* (a), *Y* и *Z* (b), and *X* и *Z* (c).

2.2. Forming the finite-element model and iterative problem solution process

Let us discretise the bar system S using the concept of the finite element method within the displacement method based on approximations used in [8, 10]. We will consider the next scheme of the description of displacements in the bar finite element of bar T (see Fig. 2). Let us represent the vector of generalised strains of the finite element as follows:

$$\left\{\varepsilon_e\right\} = \left\{\varepsilon_x \quad \chi_y \quad \chi_z \quad \theta \quad \frac{\partial\theta}{\partial x}\right\}^T. \tag{6}$$

Vector of generalised stresses corresponding to vector $\{\varepsilon\}$

$$\left\{\sigma_e\right\} = \left\{N \quad M_y \quad M_z \quad M_\theta \quad B_\omega\right\}^T. \tag{7}$$

Let us set down the vector of generalised displacements of finite element node i as

$$\left\{\delta_i\right\} = \left\{u_i \quad v_i \quad w_i \quad \phi_{xi} \quad \phi_{yi} \quad \phi_{zi} \quad \theta_i\right\}^T \left(i = 1, 2\right). \tag{8}$$

Taking into account Equations (6) and (7), let us represent the finite element elasticity matrix $\left[D_e\right]$ determined by relationship $\left\{\sigma_e\right\}=\left[D_e\right]\left\{\varepsilon_e\right\}$ [35] as follows:

$$\left[D_e\right]=\mathrm{diag}\left\{EA \quad EI_y \quad EI_z \quad GI_t \quad EI_\omega\right\}, \tag{9}$$

where E, G are material elasticity modulus and shear modulus,

A is the bar cross section area,

I_y and I_z are the cross-sectional moments of inertia relative to axes Cy and Cz ,

I_t is the geometrical stiffness factor for pure torsion,

I_ω is the principal sectorial moment of inertia.

Let us approximate displacement u along axis Ox using linear law, and displacements v, w and rotation angle ϕ_x using third-degree polynomials. We represent the vector of nodal displacement of the finite element as

$$\left\{\delta_e\right\}=\begin{Bmatrix}\left\{\delta_1\right\}\\ \left\{\delta_2\right\}\end{Bmatrix}. \tag{10}$$

Then taking into account Equations (6), (8), and (10), let us report the finite element strain matrix $\left[B_e\right]$ determined by expression $\left\{\varepsilon_e\right\}=\left[B_e\right]\left\{\delta_e\right\}$ [35] in terms of

$$\left[B_e\right]=\left[\left[B_{e1}\right] \quad \left[B_{e2}\right]\right], \tag{11}$$

where

$$\left[B_{e1}\right]=\begin{bmatrix} -\frac{1}{l} & 0 & 0 & 0 & 0 & 0 & 0 \\ 0 & 0 & \frac{6}{l^2}-\frac{12x}{l^3} & 0 & -\frac{4}{l}+\frac{6x}{l^2} & 0 & 0 \\ 0 & \frac{6}{l^2}-\frac{12x}{l^3} & 0 & 0 & 0 & \frac{4}{l}-\frac{6x}{l^2} & 0 \\ 0 & 0 & 0 & -\frac{6x}{l^2}+\frac{6x^2}{l^3} & 0 & 0 & 1-\frac{4x}{l}+\frac{3x^2}{l^2} \\ 0 & 0 & 0 & -\frac{6}{l^2}+\frac{12x}{l^3} & 0 & 0 & -\frac{4}{l}+\frac{6x}{l^2} \end{bmatrix},$$

$$\left[B_{e2}\right]=\begin{bmatrix} \frac{1}{l} & 0 & 0 & 0 & 0 & 0 & 0 \\ 0 & 0 & -\frac{6}{l^2}+\frac{12x}{l^3} & 0 & -\frac{2}{l}+\frac{6x}{l^2} & 0 & 0 \\ 0 & -\frac{6}{l^2}+\frac{12x}{l^3} & 0 & 0 & 0 & \frac{2}{l}-\frac{6x}{l^2} & 0 \\ 0 & 0 & 0 & \frac{6x}{l^2}-\frac{6x^2}{l^3} & 0 & 0 & -\frac{2x}{l}+\frac{3x^2}{l^2} \\ 0 & 0 & 0 & \frac{6}{l^2}-\frac{12x}{l^3} & 0 & 0 & -\frac{2}{l}+\frac{6x}{l^2} \end{bmatrix}.$$

Let us calculate the finite element stiffness matrix using numerical integration based on Gaussian quadrature on three points. In such a case, if an auxiliary variable $\zeta = 2(x - l/2)/l$ is used, it can be set down as

$$\left[K_e\right] = \frac{l}{2} \sum_{j=1}^{3} \psi_j \left[B_e\left(\zeta_j\right)\right]^T \left[D_e\right]\left[B_e\left(\zeta_j\right)\right], \tag{12}$$

where $\psi_1 = \psi_3 = 5/9$, $\psi_2 = 8/9$, $\zeta_1 = -\zeta_3 = \sqrt{0.6}$, $\zeta_2 = 0$ are coefficients and coordinates of Gaussian integration points.

When a finite element system is formed, one should transfer to nodal points in bending centers P_i. Let us note the correctness of the equality

$$u_i = u_{Pi} + \phi_{zi} f_y - \phi_{yi} f_z, \tag{13}$$

where u_{Pi} is the projection of the displacement vector of cross section H_i bending center on axis Ox;

f_y, f_z are the projections of vector $\vec{f}$ on axes Oy and Oz (see Fig. 2).

Taking into account Equations (8) and (13), let us express vector $\left\{\delta_i\right\}$ through vector $\left\{\delta_{Pi}\right\}$ of generalized displacements for node in the point P_i:

$$\left\{\delta_i\right\} = \left[\Delta\right]\left\{\delta_{Pi}\right\}, \tag{14}$$

where

$$\left[\Delta\right] = \begin{bmatrix} 1 & 0 & 0 & 0 & -f_z & f_y & 0 \\ 0 & 1 & 0 & 0 & 0 & 0 & 0 \\ 0 & 0 & 1 & 0 & 0 & 0 & 0 \\ 0 & 0 & 0 & 1 & 0 & 0 & 0 \\ 0 & 0 & 0 & 0 & 1 & 0 & 0 \\ 0 & 0 & 0 & 0 & 0 & 1 & 0 \\ 0 & 0 & 0 & 0 & 0 & 0 & 1 \end{bmatrix},$$

$$\left\{\delta_{Pi}\right\} = \left\{u_{Pi} \quad v_i \quad w_i \quad \phi_{xi} \quad \phi_{yi} \quad \phi_{zi} \quad \theta_i\right\}^T \left(i = 1, 2\right).$$

Then the finite element stiffness matrix for nodal points in bending centers will be determined by relationship

$$\left[K_{Pe}\right] = \left[\Omega\right]^{-1}\left[K_e\right]\left[\Omega\right], \tag{15}$$

where matrix

$$\left[\Omega\right] = \begin{bmatrix} \left[\Delta\right] & 0 \\ 0 & \left[\Delta\right] \end{bmatrix}.$$

Taking into account Equations (1), (2), (10), (14), and (15), the system of equations for the finite element formed on the basis of the variational principle of Lagrange can be represented a follows:

$$\left(\left[K_{pe}\right]\left\{\delta_{Pe}\right\}\right)^* = \left(\left[\Omega\right]^{-1}\left\{Q_e\right\} + \left\{R_{BM}\right\} + \left\{R_e\right\}\right)^*, \tag{16}$$

where $\left\{\delta_{Pe}\right\}$ is the finite element displacement vector for nodes in points P_i:

$$\left\{\delta_{Pe}\right\}=\begin{Bmatrix}\left\{\delta_{P1}\right\}\\ \left\{\delta_{P2}\right\}\end{Bmatrix},$$

$$\left\{Q_e\right\}=\left\{R_{x1}\quad R_{yi}\quad R_{zi}\quad m_{x1}\quad m_{y1}\quad m_{zi}\quad \tilde{B}_{\omega 1}\quad R_{y2}\quad R_{y2}\quad R_{y2}\quad m_{x2}\quad m_{x2}\quad m_{z2}\quad \tilde{B}_{\omega 2}\right\}^T,$$

$$\left\{R_{BM}\right\}=\left\{0\quad 0\quad 0\quad 0\quad 0\quad 0\quad B_{M\omega 1}\quad 0\quad 0\quad 0\quad 0\quad 0\quad 0\quad B_{M\omega 2}\right\}^T,$$

$$B_{M\omega i}=B_{\omega}\left(m_{yi}\right)+B_{\omega}\left(m_{zi}\right)\ (i=1,2),$$

$\left\{R_e\right\}$ is the vector of parts of external nodal forces applied in cross sections H_1, H_2.

Taking into account relationships (5) and (16) let us set down the system of linear algebraic equations for the finite-element model of bar system as

$$\left(\left[K\right]\left\{\delta\right\}\right)^*=\left(\left\{R_{BM}\right\}+\left\{R\right\}\right)^*, \tag{17}$$

where $\left[K\right]$ is the global stiffness matrix,

$\left\{\delta\right\}$ is a vector of nodal displacement of the finite-element model,

$\left\{R_{BM}\right\}$ is a vector formed on the basis of bimoments $B_{\omega}\left(m_{yi}\right)$ and $B_{\omega}\left(m_{zi}\right)$,

$\left\{R\right\}$ is a vector of external generalized nodal forces.

Let us introduce the following iterative process for solution the system of Equations (17):

$$\left[K\right]\left\{\delta\right\}^{(s)}=\left\{R\right\}+\left\{R_{BM}\right\}^{(s-1)}\left(s=1,2\,..\right), \tag{18}$$

where s is an iteration number,

$\left\{R_{BM}\right\}^{(s-1)}$ is the vector $\left\{R_{BM}\right\}$ obtained from the results of iteration $s-1$ with $\left\{R_{BM}\right\}^{(0)}=0.$

As shown by calculations, iterative process (18) usually practically converges on highest values of internal force factors in 3 to 6 iterations. In the first iteration one can perform LU decomposition [36] the matrix of system of equations. Then contribution of subsequent iterations into the overall labor intensity of the solution of the problem will be insignificant.

3. Results and Discussion

Let us provide the results of the calculations using the suggested methodology for two examples. In example 1 a steel deformable system formed by bars I and II was considered (Fig. 6). Bar I is made of I-section No. 20B1 according to Russian State Standard GOST R 57837-2017, bar 2 is made of channel section No. 10P according to Russian State Standard GOST 8240-97. The bars have transversal ribs R. The system has rigid fixing H and loading with force couple with moment M. This object was calculated using a shell finite element model (Fig. 7) in the finite element analysis program Autodesk NEi Nastran (license of Federal State Budget Educational Institution of Higher Education “Bryansk State Engineering Technological University”, No. PR-05918596) and using a bar model (Fig. 8). 6450 quadrangular shell-type finite elements and 10 thin-walled bar finite elements were considered, respectively. Further refinement of both meshes did not lead in any significant changes of the calculation results. Fig. 9 illustrates a diagram of bimoments in bars obtained using a shell model. Fig. 10 and 11 illustrate bimoments calculated using the considered bar finite element without adjustment on bimoments and with implementation of the iterative process (18). Here the signs of bimoments correspond to local coordinate systems $x_i y_i z_i$ $\left(i=\mathrm{I},\mathrm{II}\right)$ for the beams (see Fig. 6). For the shell model, during calculation of bimoments according to Fig. 4 and 12 an approximate relationship was used

$$B_{\omega}=\sum_{j=1}^{n}\sigma_j t_j l_j \omega_j, \tag{19}$$

where n is the number of finite elements separated by the cross section in question into line segments Λ_i of its middle surfaces,

σ_j is the membrane stress for this cross section in finite element j averaged on line segment Λ_j,

t_j is the thickness of finite element j,

l_j is the length of line segment Λ_j,

ω_j is the principal sectorial coordinate of the center of this line segment.

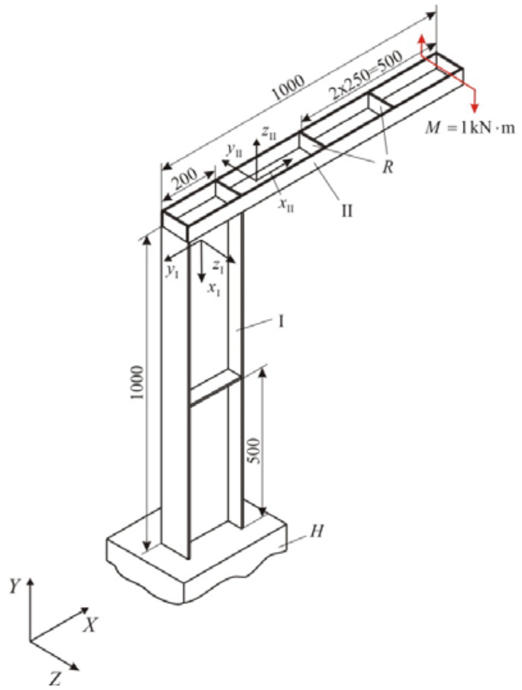

Figure 6. Double-bar system.

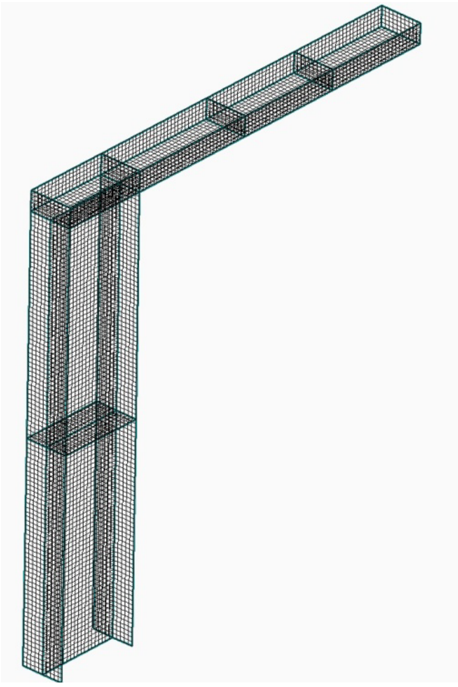

Figure 7. System of shell finite elements for example 1.

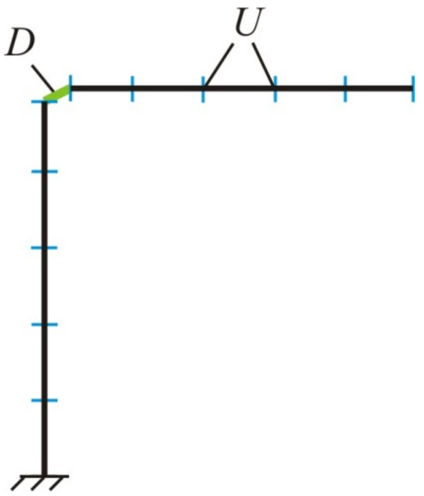

Figure 8. Splitting of example 1 object into bar finite elements: U are the finite element nodes.

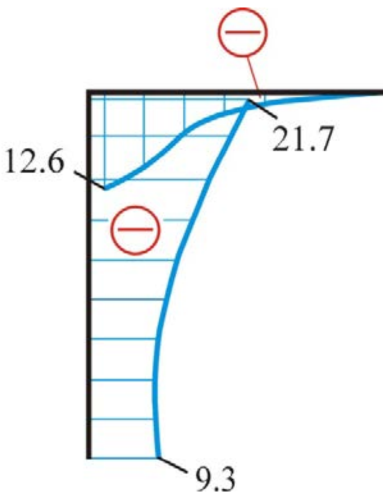

Figure 9. Diagram of bimoments according to calculation results in Autodesk NEi Nastran (N·m^2).

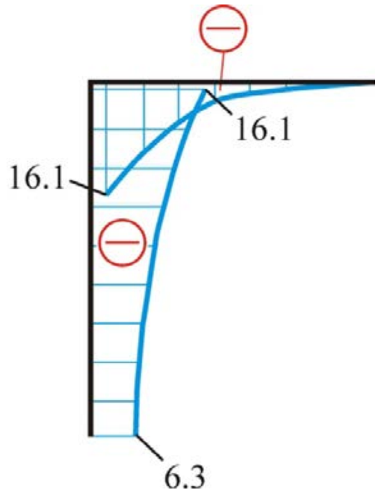

Figure 10. Bimoment calculation results for bar model without considering the disturbance on bimoments (N·m^2).

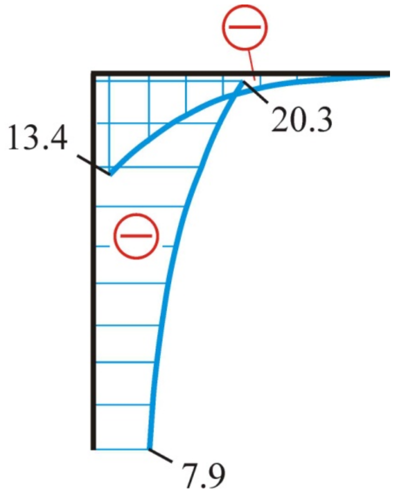

Figure 11. Diagram of bimoments obtained upon introduction of correcting nodal bimoments (N·m^2).

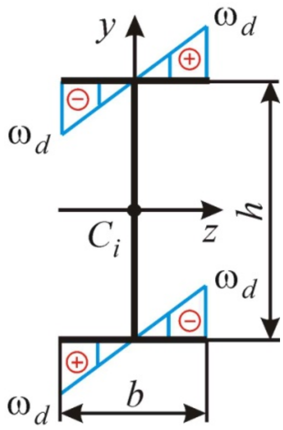

Figure 12. Principal sectorial coordinates for I-section: ω_d is a value depending on the dimensions of the cross section.

Fig. 9–11 show that on the maximum absolute value of bimoment in I-section the result obtained in the bar model without implementation of iterative process (18) is different from the shell model by 26 %, and on bimoment in channel section by 28 %. When the correcting bimoments were used, the respective discrepancies amounted only 6.5 % and 6.3 %. Fig. 13 illustrates the graphs of the behavior of these bimoments during the iterative process. It shows that the convergence on them is actually achieved in 3 iterations.

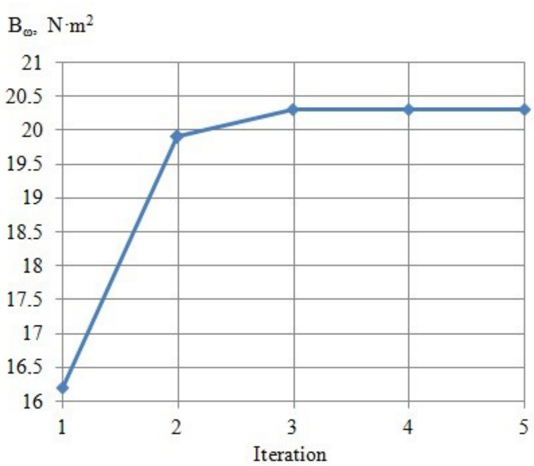

a.

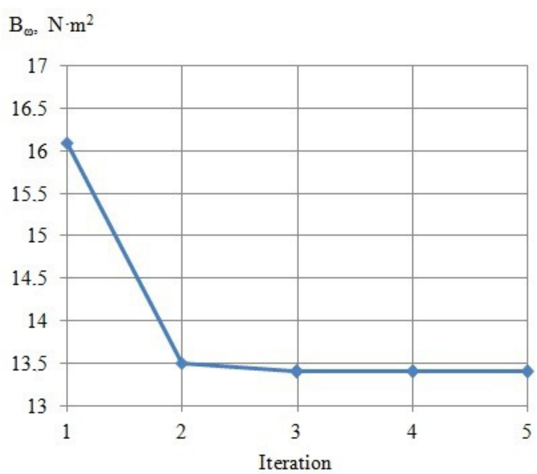

b.

Figure 13. Bimoments in example 1 for the joined node in I-section (a) and channel section (b) depending on the iteration number.

In example 2 the steel frame (Fig. 14) is calculated. Its columns are channel sections, and the cross bar is I-section. The dimensions of cross sections are assumed to be the same as for the dimensionally identical sections in example 1. The bars are reinforced with transversal ribs R. The columns are fixed rigidly at the bottom in supports H. The system is loaded with moments M_1, M_2, M_3, concentrated forces F_1, F_2, F_3, acting in the median planes of the channel webs, and distributed load q, acting in the main vertical plane of the crossbar.

The calculation results were compared using shell and bar models. For the shell scheme (Fig. 15) 31,850 finite elements were used. When the bar model was formed, 92 thin-walled bar finite elements were introduced. By analogy with example 1, the results of the calculation of bimoments using Autodesk NEi Nastran are provided in Fig. 16. The bimoments obtained for the bar model based on iterative adjustment are shown in Fig. 17. The signs of bimoments in these diagrams were assumed in accordance with the position of the local coordinate axes shown in Fig. 14. Comparing Fig. 16 and 17 one can conclude that in terms of the bimoment value maximum for joined nodes, the result obtained using the suggested methodology is different from the shell model by 6.6 %, and in terms of the maximum value of bimoment in the columns, by 5.2 %. The bimoment values calculated in the iterative process for joined node A are shown in Fig. 18, where it is clear that in terms of these magnitudes, the convergence was actually achieved in 4 to 6 iterations.

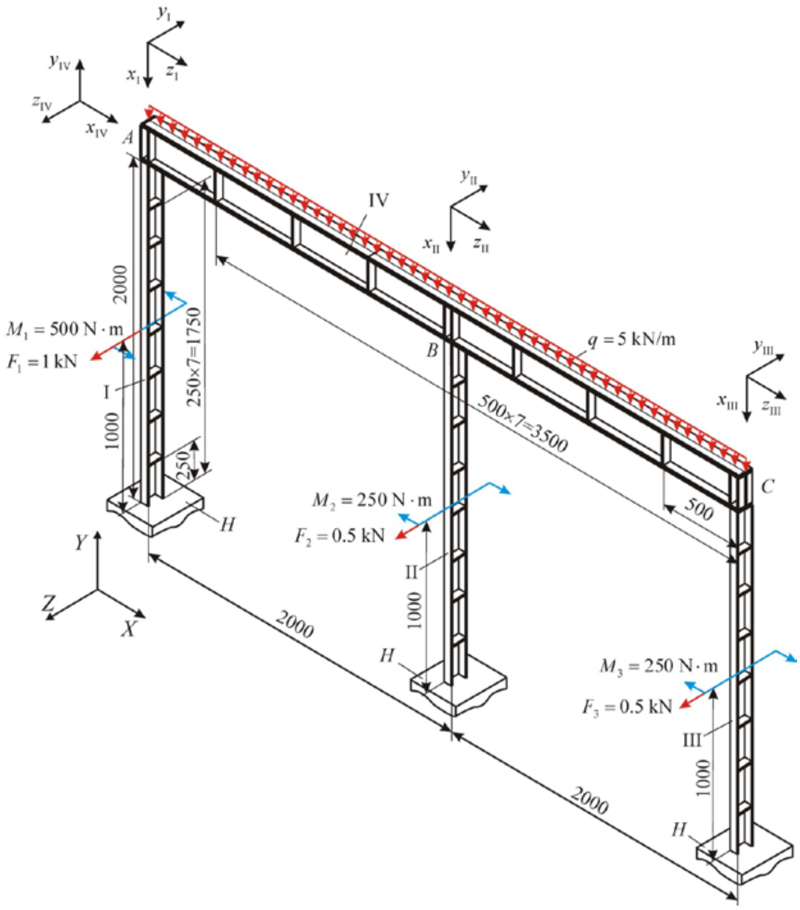

Figure 14. Double-span frame: I, II, III are the structurally identical columns; IV is the cross bar; *A*, *B*, *C* are the bar connection nodes.

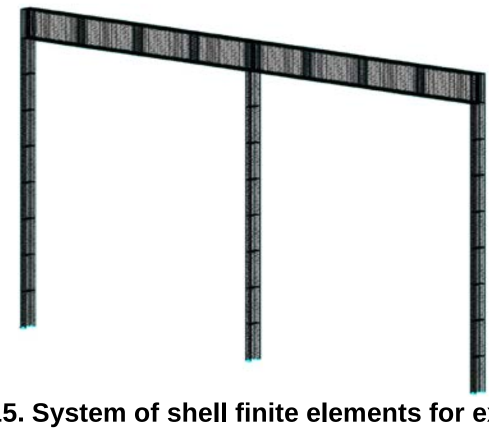

Figure 15. System of shell finite elements for example 2.

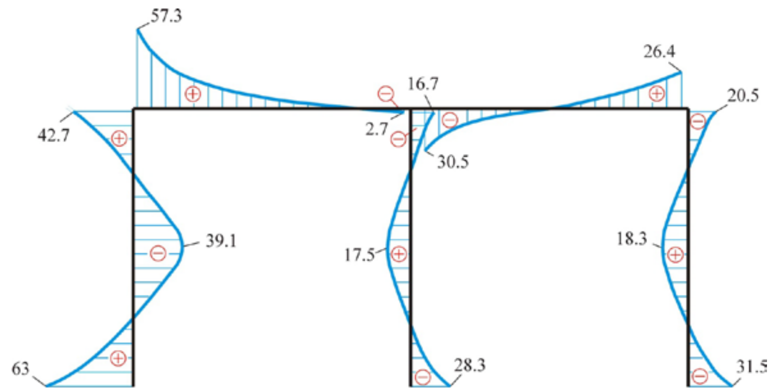

Figure 16. The results of bimoments calculation based on the shell model (N·m²).

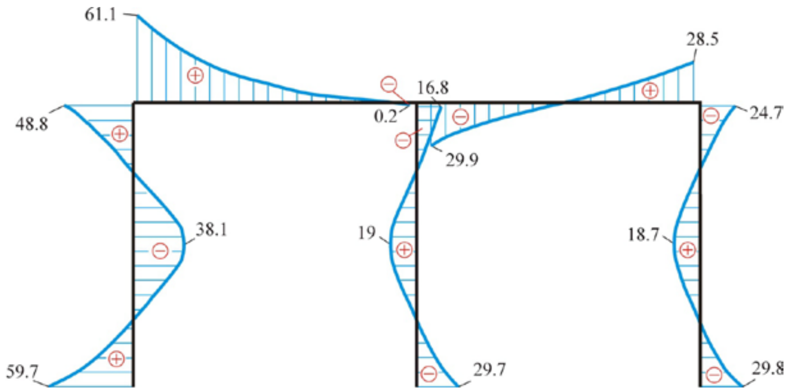

Figure 17. The results of bimoments calculation using a correcting iterative scheme in the bar model (N·m²).

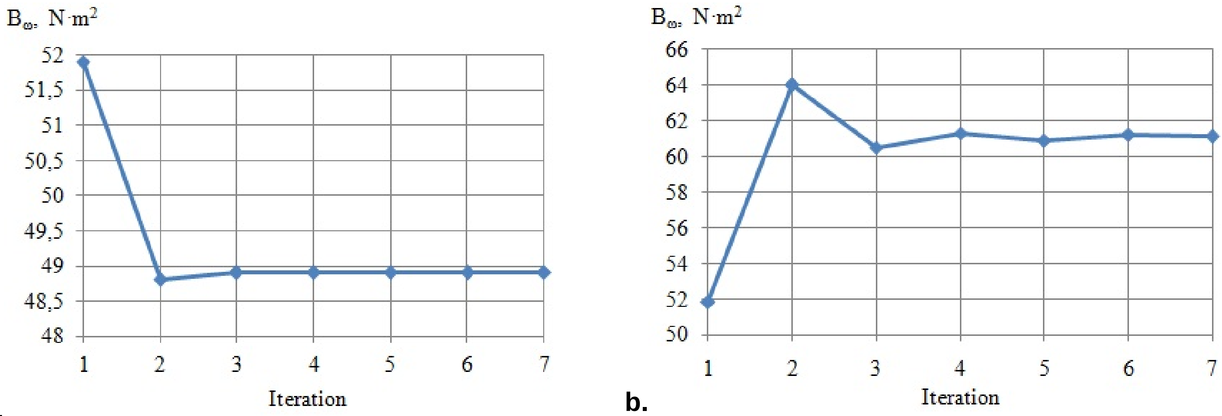

a. **b.**

Figure 18. The change of bimoments of node *A* for column (a) and cross bar (b) in the iterative process.

It should be noted that in the structures where the bar connection nodes have significant reinforcement, including that using inclined ribs, some additional disturbances in terms of bimoments may appear. At the same time, such disturbance types may appear also in some straight bars if there are any design factors determining the local restrained warpings [5]. In such cases, in addition to the suggested approach, both for frames and individual bars, it is necessary to introduce into the design model some stiffening elements resistant to the bimoment transfer. According to [33, 34], when using only transversal ribs with thickness in accordance with the requirements of Russian State Standard SP 16.13330.2017, such additional disturbances are insignificant. At the same time, as follows from results of the presented work, when the bar models are used, taking into account the disbalance on bimoments in bar connection nodes caused by moment transfer behavior can increase the calculation precision significantly.

4. Conclusions

1. An algorithm of correcting bimoments has been developed. It allows taking into account the disbalance on bimoments in joined nodes of frames which are generated via open-section bars equipped with transversal ribs based on a rapidly converging iterative process. In this calculation scheme, the same matrix

of system of equations is used during each iteration. It determines the main labor intensity of the calculation process for execution of the first iteration.

2. Strains of each bar are simulated within V.Z. Vlasov's shearless theory. Based on the approach of V.V. Lalin and V.A. Rybakov, stiffness matrices have been constructed for double-node bar finite elements in which the cross section rotation angles are described using cubic law.

3. Using the variational principle of Lagrange and taking into account the conditions of the moment transfer at bar junctions, the finite element method resulting system of equations is formed. It includes the global stiffness matrix constructed in the supposition of the bimoment balance in the bar connection nodes, and on the right hand side of the equations, the correcting bimoments are included. They are determined during iterations.

4. The results are provided for finite element method calculation on bimoment values for two frames using shell models and the suggested algorithm. When corrective bimoments were used, the iterative process practically converged in 3 to 6 iterations. Herewith, the deviation of the calculation results in the presented bar models as compared with the shell schemes amounted to no more than 7 % of the maximum absolute bimoment values.

5. Acknowledgement

The reported study was funded by RFBR according to the research project No. 18-08-00567.

References

1. Gordeeva, A.O., Vatin, N.I. Raschetnaya konechno-elementnaya model' kholodnognutogo perforirovannogo tonkostennogo sterzhnya v programmno-vychislitel'nom komplekse SCAD Office [Finite element calculation model of thin-walled cold-formed profile in software package SCAD Office]. Magazine of Civil Engineering. 2011. 21(3). Pp. 36–46. (rus). DOI: 10.18720/MCE.21.2
2. Kvaternik, S., Turkalj, G., Lanc, D. Analysis of flexure, torsion and buckling of thin-walled frames with a focus on the joint warping behaviour. Transactions of FAMENA. 2018. 41(4). Pp. 1–10. DOI: 10.21278/TOF.41401
3. Tusnina, O.A. Finite element analysis of crane secondary truss. Magazine of Civil Engineering. 2018. 77(1). Pp. 68–89. DOI: 10.18720/MCE.77.7
4. Bernardo, L.F.A., Taborda, C.S.B., Andrade, J.M.A. Ultimate torsional behaviour of axially restrained RC beams. Computers and Concrete. 2015. 16(1). Pp. 67–97. DOI: 10.12989/cac.2015.16.1.067
5. Vlasov, V.Z. Tonkostennyye uprugiye sterzhni [Thin-walled elastic rods]. Gosudarstvennoye izdatel'stvo fiziko-matematicheskoy literatury. Moscow, 1959. 568 p. (rus)
6. Bychkov, D.V. Stroitel'naya mekhanika sterzhnevykh tonkostennykh konstruktsiy [Structural mechanics of rod thin-walled structures] / D.V. Bychkov. Gosudarstvennoye izdatel'stvo literatury po stroitel'stvu, arkhitekture i stroitel'nym materialam. Moscow, 1962. 476 p. (rus)
7. Slivker, V.I. Stroitel'naya mekhanika. Variatsionnyye osnovy [Structural mechanics. Variational bases]. Izdatel'stvo Assotsiatsii stroitel'nykh vuzov. Moscow, 2005. 736 p. (rus)
8. Lalin, V.V., Rybakov, V.A. Konechnyye elementy dlya rascheta ograzhdayushchikh konstruktsiy iz tonkostennykh profiley [The finite elements for design of building walling made of thin-walled beams]. Magazine of Civil Engineering. 2011. 26(8). Pp. 69–80. (rus). DOI: 10.5862/MCE.26.11
9. Lalin, V.V., Rybakov, V.A., Morozov, S.A. Issledovaniye konechnykh elementov dlya rascheta tonkostennykh sterzhnevykh sistem [The finite elements research for calculation of thin-walled bar systems]. Magazine of Civil Engineering. 2012. 27(1). Pp. 53–73. (rus). DOI: 10.5862/MCE.27.7
10. Serpik, I.N., Shvyryaev, M.V. Finite element modeling of operation for thin-walled open cross section bars to analyze plate-rod systems. Russian Aeronautics. 2017. No. 60. Pp. 34–43. DOI: 10.3103/S1068799817010068
11. Serazutdinov, M.N., Ubaydulloyev, M.N., Sagdatullin, M.K. Variatsionnyy metod rascheta napryazhenno-deformirovannogo sostoyaniya tonkostennogo sterzhnya otkrytogo profilya [Variational method for calculating the stress-strain state of a thin-walled open-profile rod]. Vestnik Kazanskogo Tekhnologicheskogo Universiteta. 2014. 17(8). Pp. 255–259. (rus)
12. Rybakov, V.A., Gamayunova, O.S. Napryazhenno-deformirovannoye sostoyaniye elementov karkasnykh sooruzheniy iz tonkostennykh sterzhney [The stress-strain state of frame constructions' elements from thin-walled cores]. Construction of Unique Buildings and Structures. 2013. 12(7). Pp. 79–123. (rus). DOI: 10.18720/CUBS.12.10
13. Tusnin, A. Finite element for calculation of structures made of thin-walled open profile rods. Procedia Engineering. 2016. No. 150. Pp. 1673–1679. DOI: 10.1016/j.proeng.2016.07.149
14. Tusnin, A.R. Konechnyy element dlya chislennogo rascheta konstruktsiy iz tonkostennykh sterzhney otkrytogo profilya [Finite element for numeric computation of structures of thin walled open profile bars]. Metal Constructions. 2009. 15(1). Pp. 73–78. (rus)
15. Gotluru, B.P., Schafer, B.W., Pekoz, T. Torsion in thin-walled cold-formed steel beams. Thin-Walled Structures. 2000. 37(2). Pp. 127–145. DOI: 10.1016/S0263-8231(00)00011-2
16. Yoon, K., Lee, P.-S. Modeling the warping displacements for discontinuously varying arbitrary cross-section beams. Computers and Structures. 2014. No. 131. Pp. 56–69. DOI: 10.1016/j.compstruc.2013.10.013
17. Panasenko, N.N., Yuzikov, V.P., Sinel'shchikov, A.V. Konechno-elementnaya model' prostranstvennykh konstruktsiy iz tonkostennykh sterzhney otkrytogo profilya [Finite element model of the spatial constructions from thin-walled open section rods]. In 2 parts. Part 2. Vestnik AGTU. Ser.: Morskaya tekhnika i tekhnologiya. 2015. No. 2. Pp. 116–128.
18. Musat, S.D., Epureanu, B.I. Study of warping torsion of thin-walled beams with closed cross-section using macroelements. Communications in Numerical Methods in Engineering. 1996. 12(12). Pp. 873–884. DOI: 10.1002/(SICI)1099-0887(199612)12:12<873::AID-CNM27>3.0.CO;2-E

19. Banić, D., Turkalj, G., Brnić, J. Finite element stress analysis of elastic beams under non-uniform torsion. Transactions of FAMENA. 2016. 40(2). Pp. 71–82. DOI: 10.21278/TOF.40206
20. Qi, H., Wang, Z., Zhang, Z. An efficient finite element for restrained torsion of thin-walled beams including the effect of warping and shear deformation. IOP Conf. Series: Earth and Environmental Science. 2019. 233(3). Pp. 032029. DOI: 10.1088/1755-1315/233/3/032029
21. Perelmuter, A.V., Slivker, V.I. Raschetnyye modeli sooruzheniy i vozmozhnost' ikh analiza [Design models of structures and the possibility of their analysis]. DMK Press. Moscow, 2011. 736 p. (rus)
22. Chen, C.H., Zhu, Y.F., Yao, Y., Huang, Y. The finite element model research of the pre-twisted thin-walled beam. Structural Engineering and Mechanics. 2016. 57(3). Pp. 389–402. DOI: 10.12989/sem.2016.57.3.389
23. Manta, D., Gonçalves, R. A geometrically exact Kirchhoff beam finite element with torsion warping. Proceedings of the 8th International Conference on Thin-Walled Structures (ICTWS 2018). Lisbon, Portugal. 2018. [Online]. System requirements: AdobeAcrobatReader. URL: https://research.unl.pt/ws/portalfiles/portal/5801579/A_geometrically_exact_Kirchhoff_beam_finite_element_with_torsion_warping.pdf (date of application: 19.02.2020)
24. Lalin, V.V., Rybakov, V.A., Diakov, S.F., Kudinov, V.V., Orlova, E.S. The semi-shear theory of V.I. Slivker for the stability problems of thin-walled bars. Magazine of Civil Engineering. 2019. 87(3). Pp. 66–79. DOI: 10.18720/MCE.87.6
25. Lalin, V., Rybakov, V., Sergey, A. The finite elements for design of frame of thin-walled beams // Applied Mechanics and Materials. 2014. No. 578–579. Pp. 858–863. DOI: 10.4028/www.scientific.net/AMM.578-579.858
26. Vatin, N.I., Rybakov, V.A. Raschet metallokonstruktsiy: sed'maya stepen' svobody [An Analysis of metal structures: the seventh degree of freedom]. StroyPROFIl'. 2007. 56(2). Pp. 60–63. (rus)
27. Yurchenko, V.V. Proyektirovaniye karkasov zdaniy iz tonkostennykh kholodnognutykh profiley v srede «SCAD Office» [Designing of steel frameworks from thin-walled cold-formed profiles in SCAD Office]. Magazine of Civil Engineering. 2010. 18(8). Pp. 38–46. (rus). DOI: 10.18720/MCE.18.7
28. Aleksandrov, A.V., Osokin, A.V., Aleksandrov, A.A. Razvitiye metoda konechnykh elementov dlya sistem tonkostennykh pryamolineynykh i krivolineynykh sterzhney [Development of the finite element method for systems of thin-walled straight and curved rods]. Academia. Architecture and Construction. 2006. No. 4. Pp. 57–61. (rus)
29. Perelmuter, A.V., Yurchenko, V.V. O raschete prostranstvennykh konstruktsiy iz tonkostennykh sterzhney otkrytogo profilya [On calculationof the spatial structures of thin-walled open section] // Structural Mechanics and Analysis of Constructions. 2012. 245(6). Pp. 18–25. (rus)
30. Atavin, I.V., Melnikov, B.E., Semenov, A.S., Chernysheva, N.V., Yakovleva, E.L. Influence of stiffness of node on stability and strength of thin-walled structure. Magazine of Civil Engineering. 2018. 80(4). Pp. 48–61. DOI: 10.18720/MCE.80.5
31. Chernov, S.A. Konechnyy element sterzhnya korobchatogo secheniya s uzlami po konturu secheniya [The finite element of the box-section rod with nodes along the section contour]. Avtomatizatsiya i sovremennyye tekhnologii. 2014. No. 2. Pp. 9–13. (rus)
32. Serpik, I.N., Shkolyarenko, R.O., Shvyryayev, M.V. Konechno-elementnoye modelirovaniye raboty sistem sterzhney dvutavrovogo profilya s uchetom stesnennogo krucheniya [Finite-element modeling of the operation of I-beam rod systems taking into account constrained torsion]. Integratsiya, partnerstvo i innovatsii v stroitel'noy nauki i obrazovanii: Sbornik materialov mezhdunarodnoy nauchnoy konferentsii [Integration, partnership and innovation in building science and education: Proceedings of the international scientific conference]. Moscow: Izdatel'stvo MGSU, 2016. Pp. 287–292. (rus)
33. Serpik, I., Shkolyarenko, R. Refinement of the accounting methodology of bi-moments transfer at the junctions of the I-section bars. IOP Conference Series: Materials Science and Engineering. 2019. 365(4). Pp. 042011. DOI: 10.1088/1757-899X/365/4/042011
34. Serpik, I.N., Shkolyarenko, R.O. Raschet sistem tonkostennykh sterzhney korytoobraznogo profilya s uchetom stesnennogo krucheniya [Calculation of thin-walled systems of channel bars taking into account the restrained torsion]. Stroitel'stvo i rekonstruktsiya. 2018. 78(4). Pp. 31–41. (rus)
35. Zienkiewicz, O.C., Taylor, R.L., Fox, D. The Finite Element Method for Solid and Structural Mechanics. Elsevier. Oxford, 2014. 672 p.
36. Meyer, C.D. Matrix Analysis and Applied Linear Algebra. SIAM. Philadelphia, 2000. 718 p.

Contacts:

Igor Serpik, inserpik@gmail.com
Roman Shkolyarenko, shkroman130@mail.ru